Radiation-induced Synthesis of Self-organized Assemblies of Functionalized Inorganic-Organic Hybrid Nanocomposites

ARTICLE *in* RSC ADVANCES · JUNE 2013

Impact Factor: 3.84 · DOI: 10.1039/C3RA41838C

RSC Advances

RSC Publishing

PAPER

Radiation-induced synthesis of self-organized assemblies of functionalized inorganic–organic hybrid nanocomposites†

Cite this: *RSC Advances*, 2013, **3**, 14406

Srabanti Ghosh,[a] Aparna Datta,[a] Nupur Biswas,[b] Alokmay Datta[b] and Abhijit Saha*[a]

Received 17th April 2013,
Accepted 10th June 2013

DOI: 10.1039/c3ra41838c

www.rsc.org/advances

We demonstrate a unique single-pot synthesis of self-organized structures of CdS/dendrimer nanocomposites having long-range correlation by adopting a radiation-induced technique. The present method has been able to produce long-range chain-like networks of CdS nanoparticles of high stability within the dendrimer matrix with particle size monodispersity ~6%, as visualized with atomic force microscopy, while individual particles are characterized by transmission electron microscopy, photoluminescence, absorption spectroscopy and dynamic light scattering. Results point to a possible mechanism of long-range self-organization from the nanometer to micrometer length scales, where the self-organization is controlled by surface functionality of the dendrimer molecule, solvent and crystal phase of the CdS nanocrystals. The present investigation opens up new potential routes to manipulate semiconductor nanocomposites for optical diagnostics and for applications that require dendrimer nanocomposites with a long-range order.

Introduction

Semiconductor–dendrimer nanocomposites (DNCs) have attracted considerable attention due to the amalgamation of the biomimetic properties of dendrimers with the excellent fluorescence properties of II–VI semiconductor nanoparticles (NPs).[1–4] Polyamidoamine (PAMAM) dendrimers are highly branched macromolecules possessing both the solvent filled interior core (nanoscale container) as well as a homogeneous, well-defined exterior surface functionality (nano-scaffold). They offer a powerful multifunctional platform for drug delivery, diagnostic imaging, and clinical immunoassays,[5–7] *etc*. DNCs hold the promise of being used as building blocks for highly ordered nanostructures including self-assembled ultrathin multilayer and smart nano-devices that would be of special interest.[8–10]

However, fabricating individual nano dimensions into more complex structures and devices is an area of great interest.[11,12] Especially for the interfacing of nanoscopic devices with the macroscopic world, a large number of hierarchical organization levels are required to be implemented and controlled to actually use such small devices. One strategy towards attaining this goal emerges from the application of self-organization and assembly concepts that are ubiquitously present in the biological world and used successfully in supramolecular chemistry.[13] Various pathways are being explored to achieve formation of assembly from several nanometers up to millimeters, such as lithography directed[14] or template-directed assembly.[15,16] Moreover, assembly can be driven by molecular recognition,[17] by electrostatic attraction[18] and by layer-by-layer assembly.[19] Nanoparticles can also be organized at interfaces like air–water interfaces[20] and liquid–liquid interfaces.[21] Most of these methods rely on the shape complementarity of the objects, the surface tension at the interface of an auxiliary liquid and the object surfaces, and specific molecular interactions between the individual objects.

The majority of DNCs synthesized so far belong to metal/dendrimer nanocomposites. Synthesis of semiconductor/dendrimer composites is still scarce. Several groups have pioneered the research on CdS/dendrimer nanocomposites. However, synthesis of DNCs in an aqueous medium is fraught with thermodynamic instability, resulting in the formation of micrometer-sized flocks and poor monodispersity[22–24] that restricts self-organization of the DNC and reduces its reproducibility and applicability.

Here we present results of the synthesis of highly stable, water soluble, monodispersed CdS/dendrimer nanocomposite assemblies through a straightforward one-pot process employing steady state gamma (γ) irradiation at room temperature and thereby utilizing radiolytically generated solvated elec-

[a]*UGC-DAE Consortium for Scientific Research, Kolkata Centre, III-LB/8 Bidhannagar, Kolkata, 700 098, India. E-mail: abhijit@alpha.iuc.res.in; Fax: +913323357008; Tel: +913323351866*

[b]*Applied Material Science Division, Saha Institute of Nuclear Physics, 1/AF Bidhannagar, Kolkata, 700 064, India*

† Electronic supplementary information (ESI) available. See DOI: 10.1039/c3ra41838c

trons to create the particles from ionic precursors and to facilitate the self-organization of DNCs in the aqueous medium. The solvated electron is one of the simplest reactive species in chemistry and biology. Electrons trapped in liquid ammonia, water, alcohols, amines and other polar liquids have been of interest in chemistry over a long time.[25,26] Solvated electrons have already been used to prepare a wide range of nanomaterials.[27–30] They are strongly reductive (reduction potential $E^0 = -2.9$ V) and can initiate many reduction reactions to generate ions, which are not possible *via* a normal chemical route.[29] In comparison with the other methods, the great advantage of the radiolytic method is that the experiment can be carried out at very mild conditions, such as ambient pressure, room temperature with restricted growth and high reproducibility. It is well known that, while discrete nanoparticles with controlled chemical compositions and shape and size distributions are readily synthesized, their assembly into well-defined superstructures amenable to practical use remains a difficult and demanding task. Our results demonstrate the use of solvated electrons to induce self-organization in the nanoscale, which, in turn, can lead to chain networking in the micrometer scale.

Materials and methods

Starburst polyamidamine (PAMAM) dendrimers, with generation G4.0 having surface amino groups and half generation 3.5 with carboxyl end groups, were purchased from Sigma-Aldrich, USA. $CdCl_2$, sodium thiosulfate ($Na_2S_2O_3$, $5H_2O$) and carbon disulfide (CS_2) were obtained from Merck, India. All chemicals used were of analytical grade or of the highest purity available. Milli-Q water (Millipore) and methanol were used as a solvent. Based on the manufacturer's value of the dendrimer weight fractions in methanol and the known dendrimer densities we prepared a dendrimer stock solution of 1.0×10^{-4} M in water.

Synthesis

For all γ-irradiation works, a ^{60}Co source at a dose rate of 115.3 Gy min^{-1} was used to generate e_{sol}^- at a rate of 3.3×10^{-5} M min^{-1} and 2.5×10^{-5} M min^{-1} in water and methanol, respectively. In a typical preparation of CdS/dendrimer nanocomposites, a 5 mL aliquot of $CdCl_2$ stock solution (2.0×10^{-2} M) in water was added to 10 mL of dendrimer solution and vigorously stirred for 2 min and subsequently, an appropriate amount of freshly prepared aqueous solution of sodium thiosulfate was added to make the final concentration of Cd^{2+} and dendrimer as 2×10^{-3} M and 1×10^{-4} M, respectively. The solution was then purged under N_2-saturated conditions and irradiated in the ^{60}Co gamma irradiation chamber. In a similar manner, CdS DNC were also synthesized in methanol using an appropriate quantity of CS_2 (5×10^{-2} M) in place of sodium thiosulfate (see ESI†). CdS/dendrimer nanocomposites were prepared by using PAMAM dendrimers with different terminal groups like amino (NH_2) and carboxyl (COOH).

The dendrimer mediated formation and growth of the CdS NPs was followed by UV-visible spectroscopy. It was observed that there was no significant change in the absorption spectral profile of the CdS nanoparticles in the dendrimer matrix for a period of one month. Unaltered absorption onset suggests that the particle size has not changed. These particles can be stored for at least one month without coagulation at room temperature. Furthermore, the solutions remained colourless with hardly any precipitation for at least 5 months storage at −10 °C in dark. An absorption spectrum of the dendrimer stabilized CdS NPs was obtained taking into account the absorption of the dendrimer at the same concentration as a blank reference.

Spectroscopy

Ultraviolet (UV)-visible (vis) absorption spectra were recorded on a Shimadzu UV-1601PC spectrophotometer. Photoluminescence measurements of the CdS NPs were monitored by a Perkin Elmer LS-55 luminescence spectrometer. Size distribution and zeta potential of the CdS/dendrimer nanocomposites were determined by dynamic light scattering spectrophotometry (Model DLS – nanoZS, Zetasizer, Nanoseries, Malvern Instruments). Samples were filtered several times through a 0.22 μm Millipore membrane filter prior to recording measurements.

Microscopy

Transmission electron microscopy (TEM) was carried out on JEOL-2010 with an acceleration voltage of 200 kV, in bright field and electron diffraction mode. A drop of the as-prepared CdS NPs solution was placed on a carbon-coated copper grid and dried before putting into the TEM sample chamber. We prepared samples for AFM by diluting the nanocomposite solutions with DI water (to PAMAM concentrations of 50 nM or less). Typically, we place 50 μL of the final solution directly onto the surface of a freshly cleaved silicon wafer. The samples are enclosed in covered Petri dishes and dried in air at room temperature for at least 10 h. Tapping-mode atomic force microscopy (AFM) measurements of the CdS/dendrimer nanocomposites were conducted in air using a Multiview 1000 Scanning Probe Microscope from Nanonics Imaging Limited, operated under ambient conditions with standard Nanonics glass tip of diameter 20 nm. AFM observations were repeated on different areas from 10 μm × 10 m to 1 μm × 1 μm of the same film. The images were obtained from at least 10 macroscopically separated areas on each sample. All images were processed using the standard procedures for AFM. AFM images consist of multiple scans displaced laterally from each other in the *y*-direction with 512 × 512 pixels. All AFM experiments were carried out under ambient laboratory conditions (about 20 °C).

Results and discussion

CdS DNCs were prepared by decomposition of aqueous sodium thiosulfate ($Na_2S_2O_3$) or methanolic carbon disulfide (CS_2), induced by gamma-irradiation to form transient S^- (see ESI†). It is important to note that solvated electrons can be generated *in situ* by radiolysis of water through irradiation

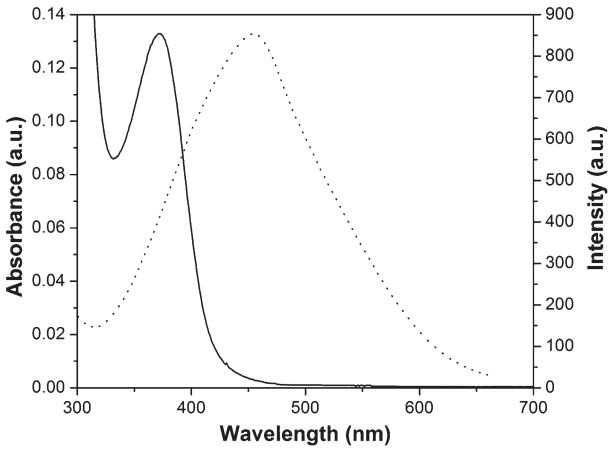

Fig. 1 Ultraviolet-visible absorption (——) and photoluminescence (·····) spectra of CdS/dendrimer nanocomposites in water using NH_2 terminated dendrimers.

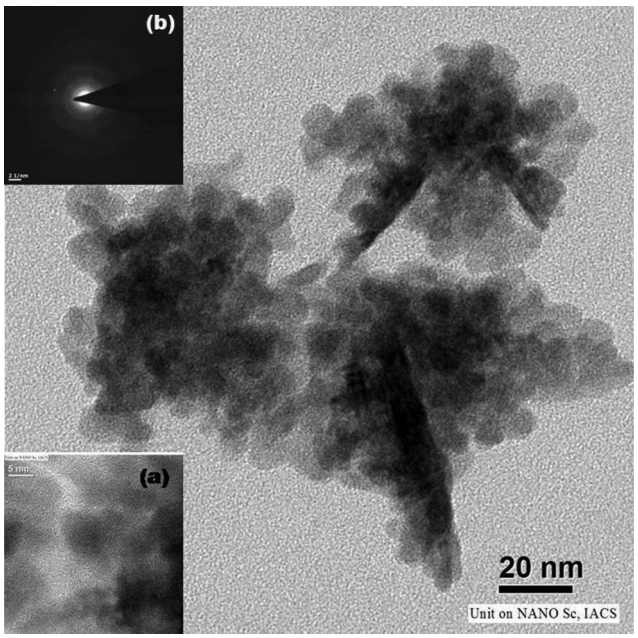

Fig. 2 Transmission Electron Microscopy image of the CdS NPs in the dendrimer (G4, NH_2 terminal) matrix in methanol. (a) High Resolution Transmission Electron Microscopy image of the CdS NPs and (b) Selected Area Electron Diffraction pattern.

with gamma irradiation, electron beams, ion beams, *etc.*, through photo-detachment of electrons from anions or by two-photon ionization of water by laser.[31] Here absorption of high energy photons by H_2O or CH_3OH generate e_{sol}^- that facilitates the generation of transient Cd^- and S^- ions which, in turn, results in CdS NPs in the dendrimer matrix. Fig. 1 illustrates a typical absorption-photoluminescence spectrum of the as-prepared CdS DNC using NH_2-terminated dendrimers in aqueous solution. The characteristic absorption and emission spectra of the CdS nanoparticles synthesized in alcoholic CS_2 medium and optical spectra (UV-vis, PL and FTIR) of DNCs are shown in the ESI† (Fig. S1 and S2–3). The excitonic absorption peak (solid) of the CdS NPs was at ~370 nm giving a narrow size distribution (~6%) while the corresponding photoluminescence peak (dashed) was at ~490 nm. The concentration of the starting materials can influence both the formation and growth of CdS nanoparticles which can be followed by UV-visible absorption and fluorescence spectroscopy. To illustrate, the effect of sodium thiosulfate concentration on the formation of CdS nanoparticles was studied with different Cd^{2+} to thiosulfate concentration ratios at a constant dose of 3.65 kGy. The UV-visible absorption profiles of the nanoparticles with a change in the Cd^{2+} : thiosulfate ratio is shown in the ESI† (Fig. S4). With an increase in the thiosulfate concentration, a red shift in the absorption onset showing an increase in particle size was observed (spectra not shown). The band gap (E_g) was calculated from absorption onset (λ_{onset}) in the UV-vis absorption spectra and the average size of the nanoparticles was obtained using the correlation of band gap shift and particle size deduced by tight-binding approximation. Further, a consistent rise in the absorption at peak around 375 nm was observed indicating an increase in the number of nanoparticles formed. The higher amount of thiosulfate would lead to greater radiolytic generation of S^- species and thus, subsequent formation of a larger number of CdS molecules is expected. It may be mentioned that changes can occur within a certain dose limit since the generation and yield of solvated electrons is governed by the absorbed radiation dose. Again, an increase in the metal : dendrimer ratio shows that although there is no significant change in absorption onset, the luminescence intensity increases with dendrimer concentration initially for the $[Cd^{2+}]$ to [dendrimer] ratio of 1 : 0.025 to 1 : 0.1 and then it decreases upon further increase of the dendrimer concentration (at 1 : 0.2). Increase in PL intensity indicates the requisite dendrimer amount for the stabilization and surface passivation of the CdS nanocrystals. The decrease in intensity could be due to structural destabilization resulting from steric hindrance at a high dendrimer concentration (ESI,† Fig. S5).

Fig. 2 shows the Transmission Electron Microscope images of the CdS NPs prepared in methanol at a typical dose of 3.46 kGy using NH_2-terminated dendrimers. Fig. 2a shows the lattice fringes indicating the crystalline structure of CdS, while Fig. 2b illustrates the corresponding selected area electron diffraction (SAED) pattern, displaying bright rings at a distance of 3.56 and 1.9 Å corresponding to the (100) and (103) lattice planes of the wurtzite crystal structure of CdS (JCPDS no. 01-0780). The presence of the rings indicates random orientations of the nanocrystals. The average size of the particles ~2.9 nm, is in good agreement with the size determined from the excitonic absorption onset following tight binding approximation.

Fig. 3a displays a typical TEM image for CdS DNC synthesized in water and Fig. 3b is the corresponding SAED. In contrast to the CdS NPs formed in methanol, indexing of

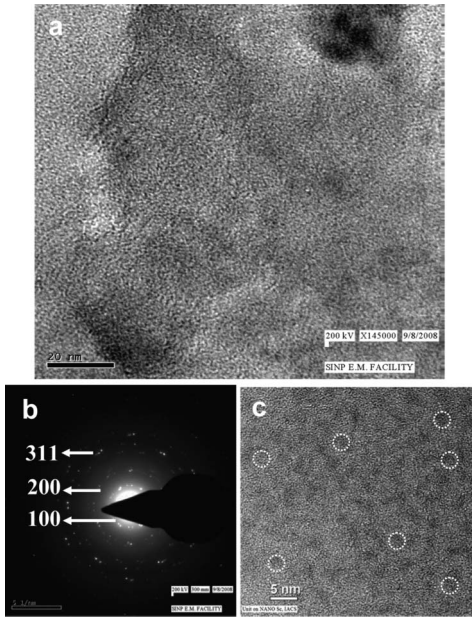

Fig. 3 Transmission Electron Microscopy image of CdS NPs in a dendrimer matrix in water (a), Selected Area Electron Diffraction pattern (b) and CdS nanocrystals marked in white (c).

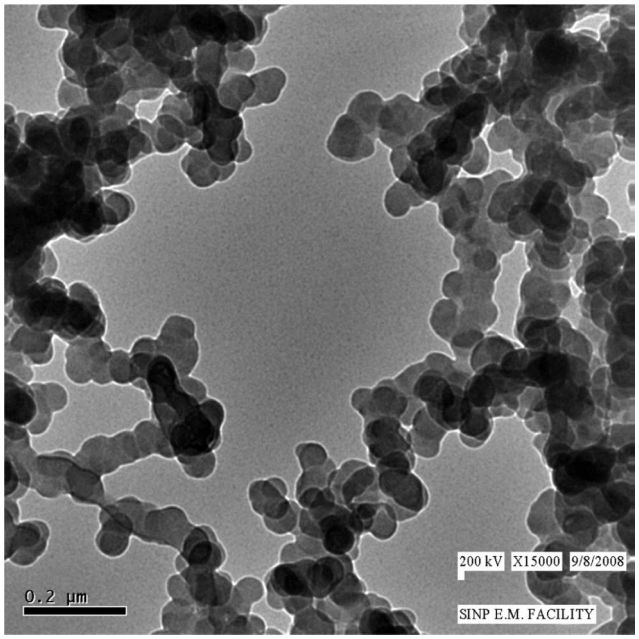

Fig. 4 Large scale Transmission Electron Microscopy image of CdS/dendrimer nanocomposites in water.

the diffraction spots confirms the (100), (200) and (311) planes of a cubic phase. More importantly, the presence of diffraction spots is a clear indication of a macroscopic orientational order in the NPs. The CdS nanocrystals are in range of 3–4 nm (marked as white circle) (Fig. 3c). The size of the nanocrystals was determined from the absorption spectral measurements as mentioned above.

The nature of this orientational order reveals itself in the lower resolution TEM image (Fig. 4), where we observe the formation of chain-like networks of semiconductor NPs in the dendrimer matrix, whereas such chains are absent in a methanolic solution of CdS DNC. Again, aqueous CdS DNC synthesized *via* a chemical, *i.e.*, non-radiolytic route does not show such chain-like organization (Fig. 5), though they do have cubic phase structures (insets (i) and (ii), Fig. 5), signifying that the presence of the cubic phase maybe necessary but may not be sufficient for nanocomposite network formation.

Atomic Force Microscopy (AFM) measurements bring out further this contrast between the morphologies of these two groups of nanoparticles in Fig. 6a and b, which show, respectively, images of nanocomposites prepared in methanolic and aqueous media. On comparison of the two images, the most significant point is that the film deposited from a methanolic solution of DNC appeared to be uniformly spread. The in-plane correlation, obtained from images of different scan-sizes, is also almost same, a confirmation of the uniformity of the film over different length scales. This, in turn, suggests a nanoparticle–substrate interaction that dominates over inter-particle forces. In contrast, the AFM image of a film from the aqueous solution using the amine-terminated dendrimer shows a chain like structure with an average length of $\sim$5.3 μm and an average height of $\sim$35 nm (Fig. S6, ESI†). Two requirements for the formation of the chain structures emerge from the observations. The aqueous solution of DNC using the carboxyl-terminated dendrimer did not show such a type of network structure (Fig. 6c), indicating

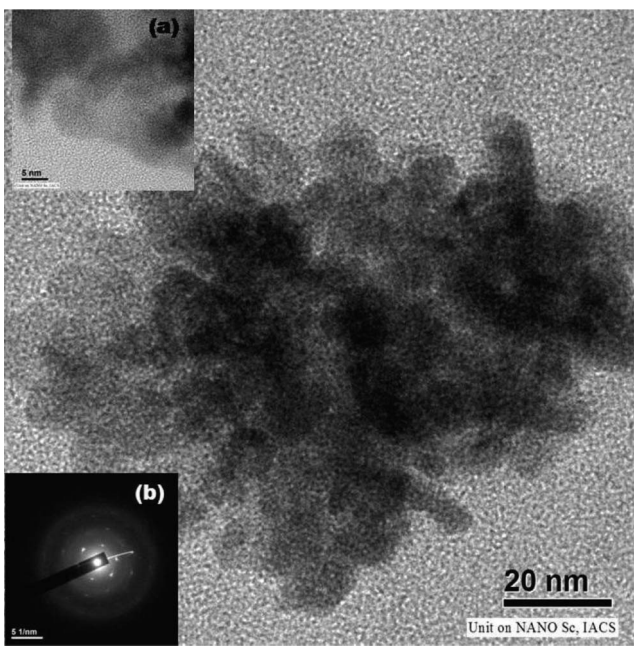

Fig. 5 Transmission Electron Microscopy image of CdS NPs prepared *via* a chemical route. Inset: (i) High Resolution Transmission Electron Microscopy image and (ii) Selected Area Electron Diffraction pattern.

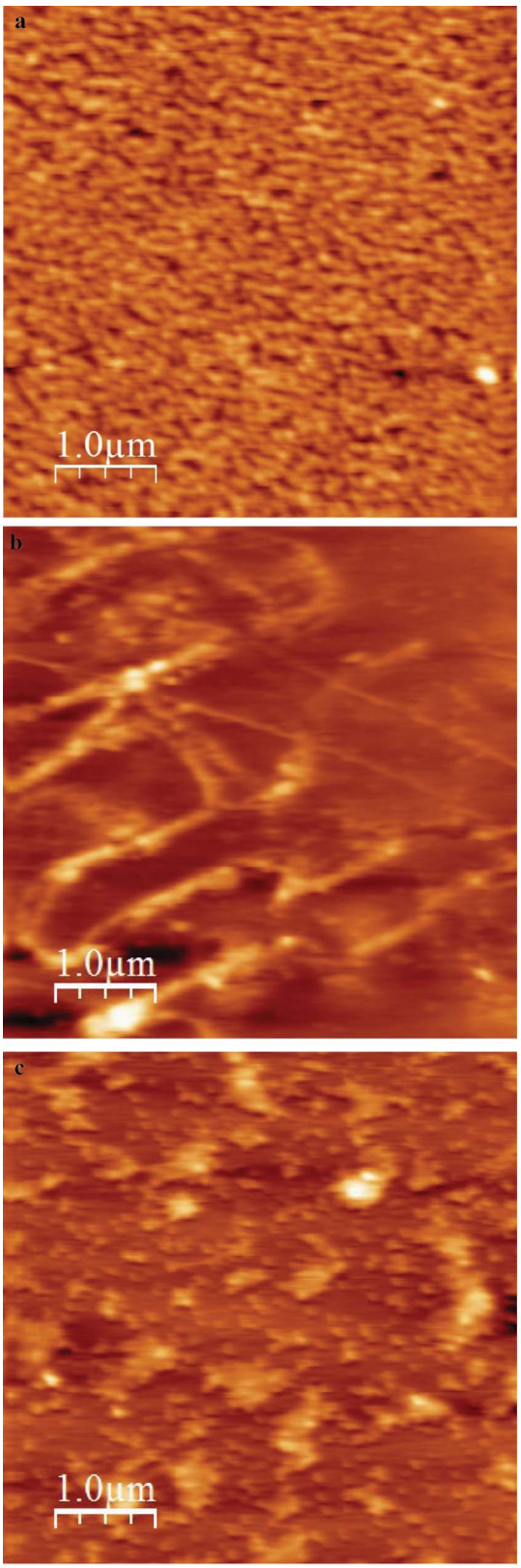

Fig. 6 Atomic Force Microscopy image of CdS/dendrimer nanocomposites in (a) methanol, (b) water using NH_2 terminated dendrimer, and (c) water using COOH terminated dendrimer.

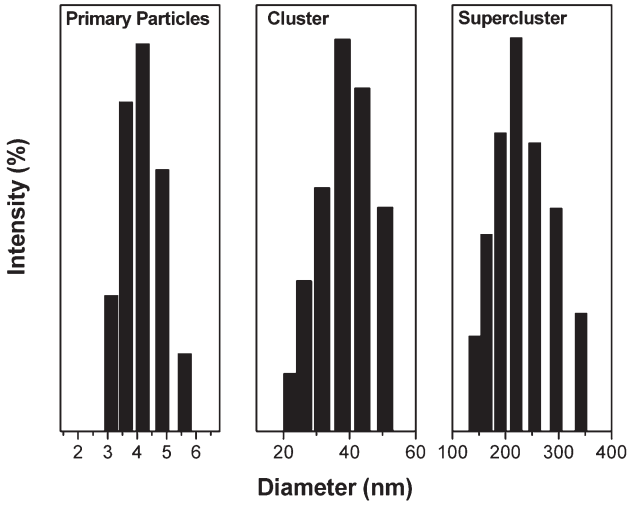

Fig. 7 Size distribution histogram of CdS/dendrimer nanocomposites by Dynamic Light Scattering (reproduced with permission from ref. 30).

that the latter occurs only in the presence of amine-terminated dendrimers. Again, this structure is observed in the dose range of 1.6–7.0 kGy and higher doses cause the disintegration of the chains.

NPs organized in such mesoscopic chains indicate the presence of a structural hierarchy spanning different length scales and this was confirmed by dynamic light scattering (DLS) of CdS DNC in aqueous media, since DLS measurements are sensitive to the size of the whole nanocomposites or association of their composites. In all samples, three length scales were found (Fig. 7, S7, ESI†), one in the scale of the NPs (median $\sim$4 nm), one in the scale of the chains (median $\sim$40 nm, consistent with the height/width of the chains) and the third in the 'super particle' scale (median $\sim$200 nm, probably a coiled state of the chain).[30]

Most nanoparticles usually do not self-assemble into their thermodynamically lowest energy state and require an input of energy or external forces to direct them into particular structures or assemblies.[32] Such anisotropic, mesoscopically correlated chain-assembly of nanocomposites rather than a homogeneous distribution of isolated nanoparticles suggests that (a) each nanoparticle associates with more than one dendrimer and, likewise, each dendrimer molecule may bind to more than one CdS NPs, *i.e.*, the driving force behind the aggregation is long-range and (b) the driving force also is anisotropic in nature. Formation of *cubic* (non-close packed) nanocrystals in aqueous media is an indication that long-range forces are present even at this initial stage and such forces may play a role in generating the long-range correlations in the 'clusters' and 'chain' hierarchies, formed in aqueous media.[33] On the other hand, the close packed wurtzite structure in the nanocrystals formed, when the synthesis was carried out in methanolic media and is characteristic of the action of short-range forces in the formation process. This is consistent with the random

orientation of the nanocrystals and the dominance of the particle–substrate forces that are essentially dipolar in nature, over particle–particle interactions. The electronic structure of hydrated electron clusters indicates that the electron distribution is localized and corresponds to an electron–ion contact pair configuration.[25] This may have implications in the interactions of hydrated electrons with Cd^{2+} ions bound with the amine-terminated dendrimer molecules.

From these results and the absence of such long-range interactions in the carboxyl-terminated dendrimers in aqueous media, we tentatively suggest that one of the differences between the NH_2- and COOH-terminals lies in the charge distribution at the dendrimer–medium interface. For both methanol and water in the presence of a carboxyl group, the density of free ions is small, intrinsically for the former (as also in the amine-terminated dendrimer in methanol) and due to the strong carboxyl–water interactions for the latter, since the carboxylic group gets dissociated. However, amine groups in presence of water do not undergo such dissociation but they protonate, and become positively charged, the amine–water interaction is weaker and hence the density of the free ions provided by water is larger. These ions can provide the long-range forces that form the cubic crystal structure. The role of water in producing cubic CdS NPs is clear by the fact that they are formed (Fig. 5) in the chemical method even when the chain-like network is absent.

As for the formation of the chain-like network, we are led to suggest that solvated electrons and the evolution of *in situ* sulfide source possibly play the major roles in this process. It is justified by the fact that solvated electrons diffuse and react with the solute by a tunnelling mechanism[34,35] facilitating the redox reaction. This enhances the reaction rate over the chemical route by a few orders of magnitude, as observed. The actual mechanism is not clear at present. Nevertheless, we tentatively suggest two factors that may play a role. One is the anisotropic environment around the dendrimer molecule having the protonated form of a terminal amine. The other is the solvated electron driven slow release of sulfide from the ionic precursor, namely, thiolate anion in the water medium. These could drive the self-organization of the correlated and anisotropic morphology as observed here.

Conclusions

Here, we have observed that a long-range self-organization from the nanometer scale to the micrometer scale is possible in the gamma radiation-induced hydrated electron mediated synthesis. The present strategy exploits the advantage of the radiation technique for controlling the slow *in situ* release of sulfide from the ionic thiosulfate during the growth of the semiconducting particles around the positively charged macromolecular structure of the dendrimer. Specifically, CdS nanocrystals in the non-characteristic cubic phase are produced, which self-organize into chain-like networks. This method may open up avenues for developing self-assembly in semiconductor nanocomposite materials.

Acknowledgements

The authors are thankful to Professor J. Belloni, France for reading this manuscript and providing valuable suggestions. Two of the authors (S. G. and N. B.) are thankful to the Council of Scientific and Industrial Research, Govt. of India, for the award of Senior Research Fellowships. The authors are also thankful to the Saha Institute of Nuclear Physics, Kolkata for providing the electron microscopy facility.

Notes and references

1 B. I. Lemon and R. M. Crooks, *J. Am. Chem. Soc.*, 2001, **122**, 12886.
2 X. C. Wu, A. M. Bittner and K. Kern, *J. Phys. Chem. B*, 2005, **109**, 230.
3 S. Ghosh, A. Priyam and A. Saha, *J. Nanosci. Nanotechnol.*, 2009, **9**, 6726.
4 S. Ghosh, A. Priyam, A. Chatterjee and A. Saha, *J. Nanosci. Nanotechnol.*, 2008, **8**, 5952.
5 D. A. Tomalia, A. M. Naylor and W. A. Goddard III, *Angew. Chem., Int. Ed. Engl.*, 1990, **29**, 138.
6 E. R. Gillies and J. M. J. Réchet, *Drug Discovery Today*, 2005, **10**, 35.
7 H. Kobayashi and M. W. Brechbiel, *Adv. Drug Delivery Rev.*, 2005, **57**, 2271.
8 W. J. Scoot, O. M. Willson and R. M. Crooks, *J. Phys. Chem. B*, 2005, **109**, 692.
9 O. V. Lebedeva, B. S. Kim, F. Gröhn and O. I. Vinogradova, *Polymer*, 2007, **48**, 5024.
10 L. Balogh, S. S. Nigavekar, B. M. Nair, W. Lesniak, C. Zhang, L. Y. Sung, W. Tan, M. S. T. Kariapper, A. El-Jawahri, M. Lanes, B. Bolton, F. Mamou, Hutson, L. Minc and M. K. Khan, *Nanomed.: Nanotechnol., Biol. Med.*, 2007, **3**, 281.
11 D. Ghosh, S. Mondal, S. Ghosh and A. Saha, *J. Mater. Chem.*, 2012, **22**, 699.
12 S. Mondal, S. Ghosh, D. Ghosh and A. Saha, *J. Phys. Chem. C*, 2012, **116**, 9774.
13 H.-P. Cong and S.-H. Yu, *Curr. Opin. Colloid Interface Sci.*, 2009, **14**, 71.
14 J. A. Liddle, Y. Cui and A. P. Alivisatos, *J. Vac. Sci. Technol., B*, 2004, **22**, 3409.
15 T. Sainsbury, T. Ikuno, D. Okawa, D. Pacilé, J. M. J. Fréchet and A. Zettl, *J. Phys. Chem. C*, 2007, **111**, 12992.
16 M. Sakurai, A. Shimojima, M. Heishi and K. Kuroda, *Langmuir*, 2007, **23**, 10788.
17 C. M. Niemeyer, *Angew. Chem., Int. Ed.*, 2001, **40**, 4128.
18 M. Sastry, M. Rao and K. N. Ganesh, *Acc. Chem. Res.*, 2002, **35**, 847.
19 A. L. Rogach, D. S. Koktysh, M. Harrison and N. A. Kotov, *Chem. Mater.*, 2000, **12**, 1526.
20 A. Swami, A. Kumar, P. R. Selvakannan, S. Mandal, R. Pasricha and M. Sastry, *Chem. Mater.*, 2003, **15**, 17.
21 A. Kumar, S. Mandal, S. Mathew, A. B. Mandale, R. V. Chaudhari and M. Sastry, *Langmuir*, 2002, **18**, 6478.

22 K. Sooklal, L. H. Hanus, H. J. Pleoehn and C. J. Murphy, *Adv. Mater.*, 1998, **10**, 1083.
23 J. R. Lakowicz, I. Gryczynski, Z. Gryczynski and C. J. Murphy, *J. Phys. Chem. B*, 1999, **103**, 7613.
24 S. K. Gayen, M. Brito, B. B. Das, G. Comanescu, X. C. Liang, M. Alrubaiee, R. R. Alfano, C. Gonzalez, A. H. Byro, D. L. V. Bauer and N. V. Balogh, *J. Opt. Soc. Am. B*, 2007, **24**, 3064.
25 J. W. T. Spinks and R. J. Woods, *Introduction to Radiation Chemistry*, third edn, New York, 1990, pp. 421–429.
26 B. Abel, U. Buck, A. L. Sobolewskic and W. Domcked, *Phys. Chem. Chem. Phys.*, 2012, **14**, 22.
27 D. Hayes, O. I. Mitit, M. T. Nenadovitt, M. T. Swayambunathan and D. J. Meisel, *J. Phys. Chem.*, 1989, **93**, 4603.
28 (*a*) J. Belloni, *Catal. Today*, 2006, **113**, 141; (*b*) J. Belloni, M. O. Delcourt and C. Leclère, *Nouv. J. Chim.*, 1982, **6**, 507.
29 A. Chatterjee, A. Priyam, S. K. Das and A. Saha, *J. Colloid Interface Sci.*, 2006, **294**, 334.
30 S. Ghosh, A. Datta and A. Saha, *Colloids Surf., A*, 2010, **355**, 130.
31 M. Spotheim-Maurizot, M. Mostafavi, T. Douki and J. Belloni, *Radiation Chemistry: from basics to applications in material and life sciences*, EDP Sciences, 2008.
32 M. C. Arsena Jr, Sauer, R. A. Crowell and I. A. Shkrob, *J. Phys. Chem. A*, 2004, **108**, 5490.
33 A. C. Ult and G. A. Ozin, *Nanochemistry: A chemical approach to nanomaterials*, Royal Society of Chemistry, Cambridge, 2005.
34 N. W. Ashcroft and N. D. Mermin, *Solid State Physics*, CBS Publishing, Philadelphia, 1988.
35 G. V. Buxton, F. C. R. Cattell and F. S. Dainton, *J. Chem. Soc., Faraday Trans. 1*, 1975, **71**, 115–122.

